

A hyper-efficient method for the analysis of pulsar timing data.

L. Lentati¹★, P. Alexander¹, M. P. Hobson¹, S. Taylor², S.T. Balan¹

¹*Astrophysics Group, Cavendish Laboratory, JJ Thomson Avenue, Cambridge, CB3 0HE, UK*

²*Institute of Astronomy, University of Cambridge, Madingley Road, Cambridge, CB3 0HA, UK*

11 October 2024

ABSTRACT

We present a new method for the analysis of pulsar timing data and the estimation of the spectral properties of an isotropic gravitational wave background (GWB). By sampling from the joint probability density of the power spectrum coefficients for the individual pulsars and the GWB signal realisation we can eliminate the most costly aspects of computation normally associated with this type of data analysis. We use a ‘Guided Hamiltonian Sampler’ to efficiently sample from this higher dimensional (~ 400) space, and show by taking this approach we need make no assumptions about the properties of the power spectrum of the GWB, thus providing a much more general approach to the problem of pulsar data analysis. When applied to the IPTA Mock Data Challenge datasets this allows us to make inferences not only on the global properties of the GWB, but also about the individual pulsars in the dataset, whilst also providing speedups of approximately two orders of magnitude.

Key words: gravitational waves – pulsars: general – methods: data analysis

1 INTRODUCTION

Millisecond pulsars (MSPs) have for some time been known to exhibit exceptional rotational stability, with decade long observations providing timing measurements with accuracies on a par with atomic clocks (e.g. Kaspi, Taylor, & Ryba 1994, Matsakis, Taylor, & Eubanks 1997). Such stability lends itself well to the pursuit of a wide range of scientific goals, e.g. observations of the pulsar PSR B1913+16 showed a loss of energy at a rate consistent with that predicted for gravitational waves (Taylor & Weisberg 1989), whilst the double pulsar system PSR J0737-3039A/B has provided precise measurements of several ‘post Keplerian’ parameters allowing for additional stringent tests of general relativity (Kramer et al. 2006).

By measuring the arrival times (TOAs) of the radio pulses to high precision it is possible to construct a timing model: a deterministic model that describes the physical properties of the pulsar e.g. its binary period and spin evolution, its trajectory, post-Keplerian terms and so on. A detailed description of this process is available in the Tempo2 series of papers (Hobbs, Edwards, & Manchester 2006, Edwards, Hobbs, & Manchester 2006, Hobbs et al. 2009). The timing model can then be subtracted from the TOAs resulting in a set of residuals which contain within them any physics not correctly accounted for by the timing model.

In this paper we will be concerned with extracting information from these residuals that results from time-correlated stochastic signals. These can include additional red noise terms due to rotational irregularities in the neutron star (Shannon & Cordes 2010) or correlated noise between the pulsars due to a stochastic gravi-

tational wave background (GWB) generated by, for example, coalescing black holes (e.g. Jaffe & Backer 2003, Phinney 2001) or cosmic strings (e.g. Kawasaki, Miyamoto, & Nakayama 2010, Ölmez, Mandic, & Siemens 2010) which could be detected using a pulsar timing array (PTA), a collection of Galactic millisecond pulsars from which the cross correlated signal induced by a GWB could be extracted. Current methods for the analysis of PTA data are for the most part extremely computationally expensive. This is particularly true for existing Bayesian methods (van Haasteren et al. (2009), van Haasteren & Levin (2012) henceforth vH2009, vHL2012) with large dense matrix inversions resulting in a scaling factor of approximately $O(n^3)$. Recently a newer method has been proposed in van Haasteren (2012) where lossy data compression is used to reduce the length of time these matrix inversions require, resulting in a speed up of ~ 3 – 6 orders of magnitude over previous methods. This method however results in extreme memory usage, and was only applied in the case where two free parameters were fitted (i.e. the amplitude and slope of a power law fitted to the GWB).

In this paper we present an alternative approach to performing a Bayesian analysis on PTA data that results in a speed up of approximately two orders of magnitude, and scales as $O(n \log(n))$ that is not limited by the number of free parameters fitted, and uses ~ 1 GB of system memory for the analysis of the IPTA Datasets. We accomplish this by rephrasing the likelihood to eliminate all matrix-matrix multiplications and costly matrix inversions, replacing them with matrix-vector operations and sparse, banded matrix inversions, whilst still retaining the ability to make robust statistical inferences about the white and red noise present in the PTA data with the same precision as in vH2009/vHL2012. We eliminate

★ E-mail: ltl21@cam.ac.uk

the need for specifying any prior form for the shape of the correlated power spectrum induced by a GWB, or the red noise present in a particular pulsar at the point of sampling, and provide a means for easily detecting bright single source objects that might affect any method that attempts to fit a prescribed model for the power spectrum, and individual pulsars that are statistical outliers within the PTA caused by unknown local effects. We perform the sampling process using a Guided Hamiltonian Sampler (GHS) (Balan, Ashdown & Hobson in prep. henceforth B12) which provides an efficient means of sampling over large numbers of dimensions (potentially $> 10^6$).

In Section 2 we describe the derivation of the new likelihood, in Section 3 we describe the sampling method used, and in Section 4 we describe the results of this method as applied to the first and second datasets from the Open IPTA Data Challenge, and make comparisons with the methods described in vHL2012.

2 ESTIMATING THE POWER SPECTRUM

For any pulsar we can write the TOAs for the pulses as a sum of both a deterministic and a stochastic component:

$$\mathbf{t}_{\text{tot}} = \mathbf{t}_{\text{det}} + \mathbf{t}_{\text{sto}}, \quad (1)$$

where \mathbf{t}_{tot} represents the n TOAs for a single pulsar, with \mathbf{t}_{det} and \mathbf{t}_{sto} the deterministic and stochastic contributions to the total respectively, where any contributions to the latter will be modelled as random Gaussian processes. In estimating the timing model parameters for the pulsar, a standard weighted least-squares fit as performed in packages such as Tempo2 will model the stochastic contributions purely as white noise characterised by the TOA uncertainties. Thus any contribution to \mathbf{t}_{sto} not described by the TOA uncertainties will be absorbed by the timing model fit and so when the timing model is subtracted from the data, any attempt to characterise the power spectrum of the resulting residuals will be incorrect.

In order to account for this, we begin by following the approach of vHL2012 which we describe in brief here so as to aid subsequent discussion. A set of pre-fit timing residuals $\delta\mathbf{t}_{\text{pre}}$ are produced using an initial estimate of the m timing model parameters β_{0i} . From here a linear approximation of the timing model can be used such that any deviations from the initial guess of the timing model parameters are encapsulated using the m parameters ϵ_i such that

$$\epsilon_i = \beta_i - \beta_{0i}. \quad (2)$$

This allows us to write the timing residuals $\delta\mathbf{t}$ in this linear approximation to the timing model as:

$$\delta\mathbf{t} = \delta\mathbf{t}_{\text{pre}} + M\boldsymbol{\epsilon} \quad (3)$$

where M is the $n \times m$ ‘design matrix’ which describes the dependence of the timing residuals on the model parameters.

We can then write the Bayesian likelihood for the timing residuals as (vH2009):

$$P(\delta\mathbf{t}|\boldsymbol{\epsilon}, \boldsymbol{\phi}) = \frac{1}{\sqrt{(2\pi)^n \det \mathbf{C}}} \exp\left(-\frac{1}{2}(\delta\mathbf{t} - M\boldsymbol{\epsilon})^T \mathbf{C}^{-1}(\delta\mathbf{t} - M\boldsymbol{\epsilon})\right) \quad (4)$$

where the $n \times n$ covariance matrix \mathbf{C} describes the stochastic contributions to the timing residuals such that

$$\langle \delta\mathbf{t}_{\text{sto}i} \delta\mathbf{t}_{\text{sto}j} \rangle = \mathbf{C}_{ij} \quad (5)$$

and is described by a set of parameters $\boldsymbol{\phi}$.

We can then marginalise over all variables $\boldsymbol{\epsilon}$ in order to calculate the probability for a particular set of parameters $\boldsymbol{\phi}$ for the stochastic contributions to the residuals, i.e.

$$P(\delta\mathbf{t}|\boldsymbol{\phi}) = \int d^m \boldsymbol{\epsilon} \frac{1}{\sqrt{(2\pi)^n \det \mathbf{C}}} \exp\left(-\frac{1}{2}(\delta\mathbf{t} - M\boldsymbol{\epsilon})^T \mathbf{C}^{-1}(\delta\mathbf{t} - M\boldsymbol{\epsilon})\right). \quad (6)$$

In vHL2012 this marginalisation is performed analytically to give:

$$P(\delta\mathbf{t}|\boldsymbol{\phi}) = \frac{1}{\sqrt{(2\pi)^{(n-m)} \det(\mathbf{G}^T \mathbf{C} \mathbf{G})}} \exp\left(-\frac{1}{2} \delta\mathbf{t}^T \mathbf{G}(\mathbf{G}^T \mathbf{C} \mathbf{G})^{-1} \mathbf{G}^T \delta\mathbf{t}\right), \quad (7)$$

where \mathbf{G} is a positive definite symmetric $n \times (n - m)$ matrix, the derivation of which will not be described here.

For the IPTA Data Challenge, data sets consisted of 130 residuals for 36 pulsars such that $n = 4680$. \mathbf{G} therefore is $\sim 4500 \times 4500$, and so the bottleneck in this calculation comes from the matrix inversion that must occur for every likelihood calculation, along with the set of matrix-matrix multiplications required to calculate $\mathbf{G}^T \mathbf{C} \mathbf{G}$.

Our goal is to remove this obstacle by rephrasing the likelihood such that 1) no matrix-matrix multiplications and 2) no computationally intensive (i.e. $O(n^3)$) matrix inversions are required in the evaluation whilst retaining the ability to accurately determine the power spectrum of the stochastic contributions to the residuals in these datasets, with a scaling of $O(n \log(n))$.

We do this first by writing our timing residuals $\delta\mathbf{t}$ as the sum of a signal \mathbf{s} that we are interested in parameterising, and some additional white noise \mathbf{n} so that we have

$$\delta\mathbf{t} = \mathbf{s} + \mathbf{n}. \quad (8)$$

We can expand \mathbf{s} in terms of its Fourier coefficients \mathbf{a} so that $\mathbf{s} = F\mathbf{a}$ where F denotes a Fourier transform. For a single pulsar the covariance matrix φ of the fourier coefficients \mathbf{a} will be diagonal, with components

$$\varphi_{ij} = \langle a_i^* a_j \rangle = \varphi_i \delta_{ij}, \quad (9)$$

where there is no sum over i , and the set of coefficients $\{\varphi_i\}$ represent the theoretical power spectrum for the residuals. When dealing with a signal from a stochastic gravitational wave background however it is crucial to include the cross correlated signal between the pulsars on the sky. We do this by using the Hellings-Downs relation (Hellings & Downs 1983):

$$\alpha_{mn} = \frac{3}{2} \frac{1 - \cos(\theta_{mn})}{2} \ln\left(\frac{1 - \cos(\theta_{mn})}{2}\right) - \frac{1}{4} \frac{1 - \cos(\theta_{mn})}{2} + \frac{1}{2} + \frac{1}{2} \delta_{mn} \quad (10)$$

where θ_{mn} is the angle between the pulsars m and n on the sky and α_{mn} represents the expected correlation between the TOAs given an isotropic background. With this addition our covariance matrix for the fourier coefficients becomes

$$\varphi_{mi,nj} = \langle a_{mi}^* a_{nj} \rangle = \alpha_{mn} \varphi_i \delta_{ij}, \quad (11)$$

where there is no sum over i , which results in a band diagonal matrix for which calculating the inverse is extremely computationally efficient.

We then sample from the joint probability density of the power spectrum coefficients and the signal realisation $\Pr(\{\varphi_i\}, \mathbf{a} | \delta\mathbf{t})$, where here \mathbf{a} refers to the concatenated vector of all coefficients a_i for all pulsars, which we can write:

$$\Pr(\{\varphi_i\}, \mathbf{a} | \delta\mathbf{t}) \propto \Pr(\delta\mathbf{t}|\mathbf{a}) \Pr(\mathbf{a}|\{\varphi_i\}) \Pr(\{\varphi_i\}) \quad (12)$$

and then marginalise over all \mathbf{a} in order to find the posterior for the parameters $\{\varphi_i\}$ alone. For our choice of $\Pr(\{\varphi_i\})$ we use a uniform prior in \log_{10} space as the scale of the coefficients is largely unknown below some upper limit, and draw from the parameter $\rho_i = \log(\varphi_i)$ instead of φ_i which has the added advantage that we avoid unnecessary rejections due to samples which have negative coefficients in the sampling process. Given this choice of prior the conditional distributions that make up Eq. 12 can be written:

$$\Pr(\delta\mathbf{t}|\mathbf{a}) \propto \frac{1}{\sqrt{\det(\mathbf{G}^T \mathbf{N} \mathbf{G})}} \times \exp\left[-\frac{1}{2}(\delta\mathbf{t} - \mathbf{F}\mathbf{a})^T \mathbf{G}(\mathbf{G}^T \mathbf{N} \mathbf{G})^{-1} \mathbf{G}^T (\delta\mathbf{t} - \mathbf{F}\mathbf{a})\right] \quad (13)$$

where $\mathbf{N} = \langle \mathbf{n}\mathbf{n}^T \rangle$ and represents the white noise errors in the residuals, which follows from Eq. 7 with \mathbf{N} replacing \mathbf{C} , and substituting $\delta\mathbf{t} - \mathbf{F}\mathbf{a}$ for $\delta\mathbf{t}$, and:

$$\Pr(\mathbf{a}|\{\rho_i\}) \propto \frac{1}{\sqrt{\det\varphi}} \exp\left[-\frac{1}{2}\mathbf{a}^{*T} \varphi^{-1} \mathbf{a}\right]. \quad (14)$$

Note that we can calculate $\mathbf{G}(\mathbf{G}^T \mathbf{N} \mathbf{G})^{-1} \mathbf{G}^T$ before the sampling starts and store it in memory which eliminates the need for any dense matrix inversions, or matrix multiplications within the likelihood calculation. It is important to state that this does not mean we are unable to fit for any of the properties of the white noise. Using the fact that \mathbf{N} is a diagonal matrix, and \mathbf{G} are block diagonal and obey the relation:

$$\mathbf{G}^T \mathbf{G} = \mathbf{I}, \quad (15)$$

the inverse term immediately simplifies to \mathbf{N}^{-1} . If we wish to model the noise for each pulsar independently, where each pulsar p has o_p residuals, m_p model fit parameters and σ_p white noise amplitude, \mathbf{N}' will be a diagonal matrix where the first $(o_1 - m_1)$ entries are equal to σ_1^2 , the next $(o_2 - m_2)$ entries will be equal to σ_2^2 and so on. Again exploiting the block diagonal nature of \mathbf{G} we can then rearrange:

$$\mathbf{G}\mathbf{N}'^{-1}\mathbf{G}^T = \mathbf{N}^{-1}\mathbf{G}\mathbf{G}^T \quad (16)$$

where we now have our original $n \times n$ matrix \mathbf{N} where the first o_1 entries are equal to σ_1^2 , the next o_2 entries will be equal to σ_2^2 and so on. For a total of n_p pulsars in the PTA data we can therefore rewrite Eq 13 as:

$$\Pr(\delta\mathbf{t}|\mathbf{a}, \{\sigma_p\}) \propto \prod_{p=1}^{n_p} \frac{1}{\sqrt{\det(\mathbf{N}_p)}} \times \exp\left[-\frac{1}{2}\mathbf{N}_p^{-1}(\delta\mathbf{t}_p - \mathbf{F}_p \mathbf{a}_p)^T \mathbf{G}_p \times \mathbf{G}_p^T (\delta\mathbf{t}_p - \mathbf{F}_p \mathbf{a}_p)\right], \quad (17)$$

where the subscript p refers to an individual pulsar in all cases. Note that we are still calculating the determinant for \mathbf{N}'_p , which is simply $\sigma_p^{(o_p - m_p)}$ rather than \mathbf{N}_p , and thus we need only store $\mathbf{G}\mathbf{G}^T$ in memory and we have eliminated any matrix-matrix multiplications, whilst still retaining the ability to fit for the noise on a per pulsar basis. As with the power coefficients φ we instead draw from the log uniform distribution $\sigma_p = 10^{2\varphi_p}$ and sample uniformly in log space.

For the sake of simplifying our notation we therefore redefine

$$\tilde{\mathbf{N}}^{-1} = \mathbf{G}\mathbf{N}'^{-1}\mathbf{G}^T. \quad (18)$$

We then draw the samples from the joint space described in equation Eq 12 using a GHS (B12) which is described in the following section.

3 GUIDED HAMILTONIAN SAMPLING

For a detailed account of both Hamiltonian Monte Carlo (HMC) and GHS refer to B12, here we will describe each only in brief. (HMC) sampling (Duane et al. 1987) has been widely applied in Bayesian computation (Neal 1993), and has been successfully applied to problems with extremely large numbers of dimensions ($\sim 10^6$ see e.g. Taylor, Ashdown, & Hobson (2008)). We define a 'potential energy' Ψ which is related to our posterior distribution $\Pr(\mathbf{x})$ by:

$$\Psi(\mathbf{x}) = -\ln(\Pr(\mathbf{x})) \quad (19)$$

where \mathbf{x} is the N dimensional vector of parameters to be sampled. Each parameter x_i must be assigned a mass m_i and a momentum p_i so that we can write our Hamiltonian as:

$$H = \sum_i \frac{p_i^2}{2m_i} + \Psi(\mathbf{x}). \quad (20)$$

The sampler is given a start point (\mathbf{x}, \mathbf{p}) and a set of momenta which are drawn from a set of N uncorrelated Gaussian distributions of width m_i in dimension i . The system can then evolve deterministically from then for some length of time τ using Hamilton's equations

$$\frac{dx_i}{dt} = \frac{\partial H}{\partial p_i}, \quad (21)$$

$$\frac{dp_i}{dt} = -\frac{\partial H}{\partial x_i} = -\frac{\partial \Psi(\mathbf{x})}{\partial x_i}. \quad (22)$$

After it has reached its new position $(\mathbf{x}', \mathbf{p}')$ that point will be accepted with a probability

$$p = \min[1, \exp(-\delta H)] \quad (23)$$

where $\delta H = H(\mathbf{x}', \mathbf{p}') - H(\mathbf{x}, \mathbf{p})$. A new set of momenta can then be drawn and the process repeats.

In order to perform the integration along the systems trajectory at each state we use a 'leapfrog' method as is common practice. Here n_s steps are taken of size λ such that $n_s \lambda = \tau$ such that:

$$p_i\left(t + \frac{\lambda}{2}\right) = p_i(t) - \frac{\lambda}{2} \frac{\partial \Psi(\mathbf{x})}{\partial x_i} \Big|_{\mathbf{x}(t)} \quad (24)$$

$$x_i(t + \lambda) = x_i(t) + \frac{\lambda}{m_i} p_i\left(t + \frac{\lambda}{2}\right) \quad (25)$$

$$p_i(t + \lambda) = p_i\left(t + \frac{\lambda}{2}\right) - \frac{\lambda}{2} \frac{\partial \Psi(\mathbf{x})}{\partial x_i} \Big|_{\mathbf{x}(t+\lambda)} \quad (26)$$

until $t = \tau$ where τ is varied to avoid resonant trajectories. HMC thus requires a large number of adjustable parameters, the mass m_i , step size λ_i and the number of steps n_s in the trajectory. Adjusting the step size or the mass produces similar effects (Neal 1996) and so one is usually fixed and the other tuned during sampling.

GHS eliminates much of this tuning aspect by using the Hessian $\hat{\mathbf{H}}$ of the joint probability distribution calculated at its peak to set the step size λ for each parameter. The masses m_i are then set to unity and the only tuneable parameter that remains is a scaling parameter η which is chosen such that the acceptance rate for the GHS is $\sim 68\%$ (see B12). Once the Hessian has been calculated, one then determines its N eigenvalues ω_i and N normalised eigenvectors \hat{e}_i .

Denoting the matrix containing these normalised eigenvectors as its columns by \mathbf{S} , one first defines a new set of variables $\mathbf{x}' = \mathbf{S}^T \mathbf{x}$ in which the Hessian becomes diagonal with the eigenvalues ω_i as its diagonal entries. One then rescales each x'_i to obtain a new set of variables $y_i = \sqrt{\omega_i} x'_i / \eta$. It is straightforward to show that the new variables are related to the original variables by

$$\mathbf{y} = \frac{1}{\eta} \hat{\mathbf{H}}^{1/2} \mathbf{x}. \quad (27)$$

Consequently, in the new variables, the Hessian at the peak has the trivial form $\eta^2 \mathbf{I}$. One then performs Hamiltonian sampling employing the standard leapfrog method, but in terms of the new variables \mathbf{y} , rather than \mathbf{x} . Thus, GHS may be considered simply as standard HMC, but performed in a set of variables (or coordinates) that are tailored to the target distribution, namely the scaled eigendirections of the Hessian at its peak. Consequently, although GHS can take advantage of a scenario where $\text{Pr}(\mathbf{x})$ possesses a single well-defined peak (with zero gradient), it does not rely on this, since it retains the generality of standard HMC.

Rather than working in terms of the new variables \mathbf{y} , one can, if desired, return to using the original variables \mathbf{x} , in which case the relation (27) shows that the leapfrog steps take the modified form

$$\mathbf{p}\left(t + \frac{\lambda}{2}\right) = \mathbf{p}(t) - \frac{\lambda}{2} \eta \mathbf{H}^{-1/2} \nabla_{\mathbf{x}} \mathcal{H} \Big|_t \quad (28)$$

$$\mathbf{x}(t + \lambda) = \mathbf{x}(t) + \lambda \eta \hat{\mathbf{H}}^{-1/2} \nabla_{\mathbf{p}} \mathcal{H} \Big|_{t+\frac{\lambda}{2}} \quad (29)$$

$$\mathbf{p}(t + \lambda) = \mathbf{p}\left(t + \frac{\lambda}{2}\right) - \frac{\lambda}{2} \eta \hat{\mathbf{H}}^{-1/2} \nabla_{\mathbf{x}} \mathcal{H} \Big|_{t+\lambda}. \quad (30)$$

Note that whilst performing the eigen-decomposition can be costly, it is only necessary to do so once at the start of the sampling where it takes ~ 10 s and is thus negligible within the scope of the sampling process as a whole. Therefore in order to perform sampling we need the following:

- The gradient of Ψ for each parameter x_i
- The peak of the joint distribution
- The Hessian at that peak

The gradients of our parameters are given by the following:

$$\frac{\partial \Psi}{\partial \mathbf{a}} = -(\delta \mathbf{t} - \mathbf{F} \mathbf{a})^T \tilde{\mathbf{N}}^{-1} \mathbf{F} + \mathbf{a}^T \varphi^{-1} \quad (31)$$

$$\frac{\partial \Psi}{\partial \Sigma_i} = \ln(10)(o_i - m_i) - \ln(10)(\delta t_i - F_i a_i)^T \tilde{\mathbf{N}}^{-1} (\delta t_i - F_i a_i) \quad (32)$$

$$\frac{\partial \Psi}{\partial \rho_i} = \frac{1}{2} \text{Tr} \left(\varphi^{-1} \frac{\partial \varphi}{\partial \rho_i} \right) - \frac{1}{2} \mathbf{a}^{*T} \varphi^{-1} \frac{\partial \varphi}{\partial \rho_i} \varphi^{-1} \mathbf{a} \quad (33)$$

and the components of the Hessian are:

$$\frac{\partial^2 \Psi}{\partial \mathbf{a}^2} = \mathbf{F}^T \tilde{\mathbf{N}}^{-1} \mathbf{F} + \varphi^{-1} \quad (34)$$

$$\frac{\partial^2 \Psi}{\partial \Sigma_i^2} = 2 \ln(10)^2 (\delta t_i - F_i a_i)^T \tilde{\mathbf{N}}^{-1} (\delta t_i - F_i a_i) \quad (35)$$

$$\frac{\partial^2 \Psi}{\partial \rho_i^2} = \mathbf{a}^{*T} \varphi^{-1} \frac{\partial \varphi}{\partial \rho_i} \varphi^{-1} \frac{\partial \varphi}{\partial \rho_i} \varphi^{-1} \mathbf{a} - 0.5 \mathbf{a}^{*T} \varphi^{-1} \frac{\partial^2 \varphi}{\partial \rho_i^2} \varphi^{-1} \mathbf{a} \quad (36)$$

$$\frac{\partial^2 \Psi}{\partial \rho_i \partial \mathbf{a}} = -\varphi^{-1} \frac{\partial \varphi}{\partial \rho_i} \varphi^{-1} \mathbf{a} \quad (37)$$

For a set of power spectrum coefficients $\{\rho_i\}$ and white noise coefficients $\{\Sigma_i\}$ we can solve for the maximum set of Fourier coefficients \mathbf{a}_{max} analytically. Rearranging Eq. 31 we find:

$$\mathbf{a}_{\text{max}} = (\mathbf{F}^T \tilde{\mathbf{N}}^{-1} \mathbf{F} + \varphi^{-1})^{-1} \mathbf{F}^T \tilde{\mathbf{N}}^{-1} \delta \mathbf{t}, \quad (38)$$

so when searching for the global maximum we need only search over the subset of parameters $\{\rho_i\}$. This is achieved by using a particle swarm algorithm (Kennedy & Eberhart 1995; 2001 and for uses in cosmological parameter estimation see e.g. Prasad & Souradeep (2012), and for a description of the particle swarm method applied to PTA data in this context see (Taylor, Gair & Lentati 2012) to efficiently find the maximum in ~ 1 minute using ~ 5 – 10 cores per free parameter. We now apply this method to the IPTA Open Datasets 1 and 2.

4 RESULTS

4.1 Open Dataset 1

The IPTA Data Challenge 1 first open dataset consists of a set of 130 timing residuals for 36 pulsars and contains only white noise with amplitude $\sigma = 100$ ns for each pulsar, and an injected GWB power spectrum with a characteristic strain spectrum given by:

$$h_c(f) = A_h \left(\frac{f}{1 \text{ yr}^{-1}} \right)^\alpha, \quad (39)$$

with A_h a dimensionless amplitude at a frequency of (yr^{-1}) and α a power law index. The parameters for the injected spectrum are $A_h = 5 \times 10^{-14}$ and $\alpha = -2/3$.

Parameterising the spectral density as in vHL2012:

$$S(f) = A^2 \left(\frac{1}{1 \text{ yr}^{-1}} \right) \left(\frac{f}{1 \text{ yr}^{-1}} \right)^{-\gamma}, \quad (40)$$

the strain spectrum will result in an observed spectral density within the residuals of:

$$S(f) = \frac{A_h^2}{12\pi^2} 1 \text{ yr}^3 \left(\frac{f}{1 \text{ yr}^{-1}} \right)^{-13/3}, \quad (41)$$

Defining $f_n = n/T$ where T is the total observation length of the dataset, we fit for the Fourier coefficients corresponding to some set $\{n\}$. The power spectrum for each of the N_p pulsars is therefore described by $2n + 1$ free parameters; the vector \mathbf{a} containing the $2n$ Fourier coefficients (n real, n imaginary) and the parameter Σ_p describing the log amplitude of the white noise. In addition we have a set of n coefficients $\{\varphi_n\}$ describing the power spectrum of the GWB, resulting in a total parameter space of $(N_p(2n + 1) + n)$ dimensions.

Those frequencies chosen to be sampled are such that when performing the search for the peak in the joint distribution the sampled set of n coefficients represent the n that contribute the greatest total power to the cross correlated spectrum. A more detailed investigation into this aspect of the sampling process will be presented in an updated version of this paper following the close of the first data challenge.

Table 1 shows a comparison of the values returned for A_h , α , the average amplitude of the white noise σ_{avg} and the run time required for convergence for different values of n , as experienced when using a single 16 core Sandy Bridge node on the high performance computer (HPC) ‘DARWIN’. We also compare this method with that described in vHL2012, running on the same system, where we are exploring a 38 dimensional parameter space using the MULTINEST algorithm (Feroz, Hobson, & Bridges 2009, Feroz & Hobson 2008) to perform parameter estimation (sampling efficiency set to 0.8 with 2000 live points).

Table 1. Comparison of sampling Methods

Method	n	A_h	α	σ_{avg} sec	Run Time
This Paper	3	$(5.1 \pm 0.5) \times 10^{-14}$	4.27 ± 0.20	$(1.20 \pm 0.03) \times 10^{-7}$	9 minutes
	4	$(5.2 \pm 0.4) \times 10^{-14}$	4.18 ± 0.18	$(1.12 \pm 0.015) \times 10^{-7}$	20 minutes
	5	$(5.09 \pm 0.27) \times 10^{-14}$	4.21 ± 0.14	$(1.06 \pm 0.03) \times 10^{-7}$	35 minutes
	6	$(5.05 \pm 0.20) \times 10^{-14}$	4.20 ± 0.12	$(1.040 \pm 0.024) \times 10^{-7}$	1 hour
vHL2012	N/A	$(4.82 \pm 0.18) \times 10^{-14}$	4.4 ± 0.08	$(0.97 \pm 0.028) \times 10^{-7}$	104 hours

From Table 1 one can see that even with as few as 3 GWB power coefficients, the constraints placed on the background are only \sim a factor 2 worse than using the method from vHL2012, and only 6 coefficients are necessary to match them. However, only when using 5+ coefficients does one also constrain the white noise to the correct value, with fewer coefficients overestimating its value by 10–20%. Run times however are dramatically lower, even in the case where 6 coefficients were used, a decrease from \sim 4 days to \sim 2 hours was observed, representing an improvement of \sim two orders of magnitude.

For the case $n = 6$ the results of parameterising the white noise coefficients $\{\Sigma_p\}$ can be seen in Fig. 1. We find an average value for the amplitude of the white noise across all pulsars, σ_{avg} , of $(1.040 \pm 0.024) \times 10^{-7}$, consistent with the data to within 2σ confidence levels.

Fig. 2 shows the 1D and 2D marginalised posteriors for the 6 fitted GWB power coefficients $\{\rho_i\}$, whilst Fig. 3 shows the power spectrum of both the coefficients $\{a\}$ for each of the 36 pulsars (red crosses), and of the GWB power coefficients $\{\rho_i\}$ (Green crosses) with the best fit single power law to the GWB coefficients overlaid as a blue dotted line. We find $A_h = (5.05 \pm 0.2) \times 10^{-14}$ and $\alpha = 4.21 \pm 0.12$, consistent with the injected spectrum at $\sim 1\sigma$ confidence levels.

4.2 Open Dataset 2

The second open data set is designed similarly to the first, with the same number of pulsars and observations and the same parameters describing the injected GWB signal. The two differences that separate the datasets is that the second dataset has uneven sampling in the time domain, and the amplitude of the white noise varies per pulsar.

For the case of $n = 10$ we show the 10 fitted GWB power coefficients (green points) with their associated errors, along with the best fit power law in Fig. 4. We find values for A_h and α of $(5.4 \pm 0.3) \times 10^{-14}$ and $\alpha = 4.30 \pm 0.12$, consistent with the injected spectrum at $\sim 1\sigma$ confidence levels.

5 CONCLUSIONS

We have investigated a new method for analysing data from a pulsar timing array that results in a speedup of approximately two orders of magnitude when compared to methods found in vHL2012 by rephrasing the likelihood function to eliminate all matrix-matrix multiplications, and costly dense matrix inversions, whilst constraining the parameters of interest within the data to the same level so that this new approach scales as $O(\log(n))$.

We have shown that in addition to providing a substantial speed up, this method offers other advantages; it does not require

any prior assumptions to be made regarding the shape of the power spectrum of the GWB signal within the data. There are also no limitations placed on the number of parameters to be fit at the point of sampling, with reasonable memory usage (\sim 1GB) and we have shown that it is robust to the presence of irregularly sampled time series data, making it suitable for real world applications.

This is made possible through the use of a ‘Guided Hamiltonian Sampler’, enabling us to efficiently sample from high-dimensional spaces (up to $\sim 10^6$), such that rather than fitting for a small number of global parameters that describe a particular model, we can simultaneously sample over the set of fourier coefficients that describe the spectrum of each pulsar individually, and also the coefficients of the GWB itself, along with any additional parameters of interest, such as the level of the white noise on a per pulsar basis. This allows us to make inferences not possible with existing methods, and as we will show in a subsequent investigation this makes it extremely robust to the presence of bright individual sources in the field, or individual pulsars that suffer from extreme local effects that might hinder methods of analysis that assume a particular model for any cross-correlated signals within the data.

6 ACKNOWLEDGEMENTS

This work was performed using the Darwin Supercomputer of the University of Cambridge High Performance Computing Service (<http://www.hpc.cam.ac.uk/>), provided by Dell Inc. using Strategic Research Infrastructure Funding from the Higher Education Funding Council for England and funding from the Science and Technology Facilities Council. We would also like to thank Rutger van Haasteren for invaluable assistance over the last few months in helping me work towards producing this manuscript.

REFERENCES

- Balan S. et al, 2012, In Prep.
- Davis M. M., Taylor J. H., Weisberg J. M., Backer D. C., 1985, Natur, 315, 547
- Duane S., Kennedy A. D., Pendleton B. J., Roweth D., 1987, PhLB, 195, 216
- Edwards R. T., Hobbs G. B., Manchester R. N., 2006, MNRAS, 372, 1549
- Feroz F., Hobson M. P., 2008, MNRAS, 384, 449
- Feroz F., Hobson M. P., Bridges M., 2009, MNRAS, 398, 1601
- Hellings R. W., Downs G. S., 1983, ApJ, 265, L39
- Hessels J. W. T., Ransom S. M., Stairs I. H., Freire P. C. C., Kaspi V. M., Camilo F., 2006, Sci, 311, 1901
- Hobbs G., et al., 2010, CQGr, 27, 084013
- Hobbs G., et al., 2009, MNRAS, 394, 1945

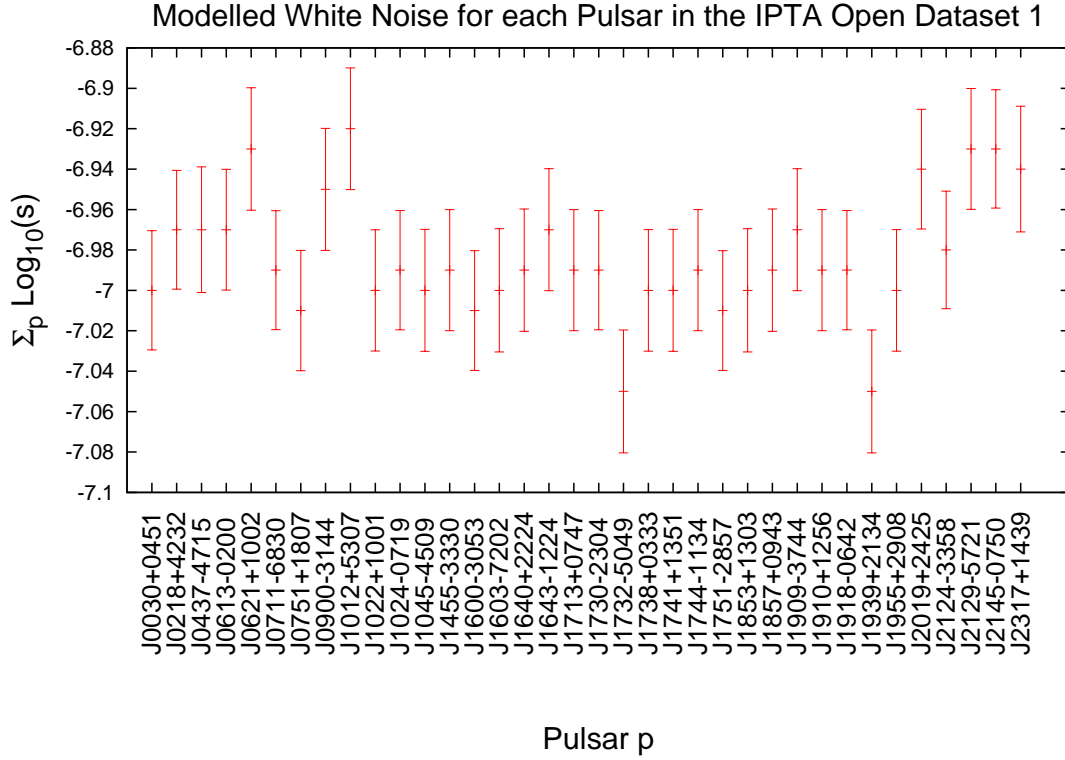


Figure 1. Parameterised values for the white noise in each pulsar in open dataset 1 from the IPTA Data Challenge. Each Pulsar has a white noise component to their residuals with an amplitude of $\sigma_p = 10^{-7}$ s. Averaging across all pulsars we find an rms value for the white noise of $\Sigma_{\text{avg}} = -6.983 \pm 0.010$ which is thus consistent with the value in the dataset to within 2σ errors.

Hobbs G. B., Edwards R. T., Manchester R. N., 2006, MNRAS, 369, 655
 Jaffe A. H., Backer D. C., 2003, ApJ, 583, 616
 Kaspi V. M., Taylor J. H., Ryba M. F., 1994, ApJ, 428, 713
 Kawasaki M., Miyamoto K., Nakayama K., 2010, PhRvD, 81, 103523
 J. Kennedy & R. C. Eberhart, 1995, IEEE Int. Conf. Neural, Networks 4, 1942
 J. Kennedy & R. C. Eberhart, 2001, Swarm Intelligence, Morgan Kufmann, San Francisco
 Kramer M., et al., 2006, Sci, 314, 97
 Matsakis D. N., Taylor J. H., Eubanks T. M., 1997, A&A, 326, 924
 Neal R., 1993, Technical report, Probabilistic Inference Using MCMCM. Department of Computer Science, University of Toronto, Toronto
 Neal R., 1996, Bayesian Learning for Neural Networks. Springer-Verlag, New York.
 Ölmez S., Mandic V., Siemens X., 2010, PhRvD, 81, 104028
 Phinney E. S., 2001, astro, arXiv:astro-ph/0108028
 Prasad J., Souradeep T., 2012, PhRvD, 85, 123008
 Shannon R. M., Cordes J. M., 2010, ApJ, 725, 1607
 Taylor J. F., Ashdown M. A. J., Hobson M. P., 2008, MNRAS, 389, 1284
 Taylor J. H., Weisberg J. M., 1989, ApJ, 345, 434

Taylor S., Gair J., Lentati L., 2012, arXiv, arXiv:submit/0571009
 van Haasteren R., Levin Y., 2012, arXiv, arXiv:1202.5932
 van Haasteren R., 2012, arXiv, arXiv:1210.0584
 van Haasteren R., Levin Y., McDonald P., Lu T., 2009, MNRAS, 395, 1005

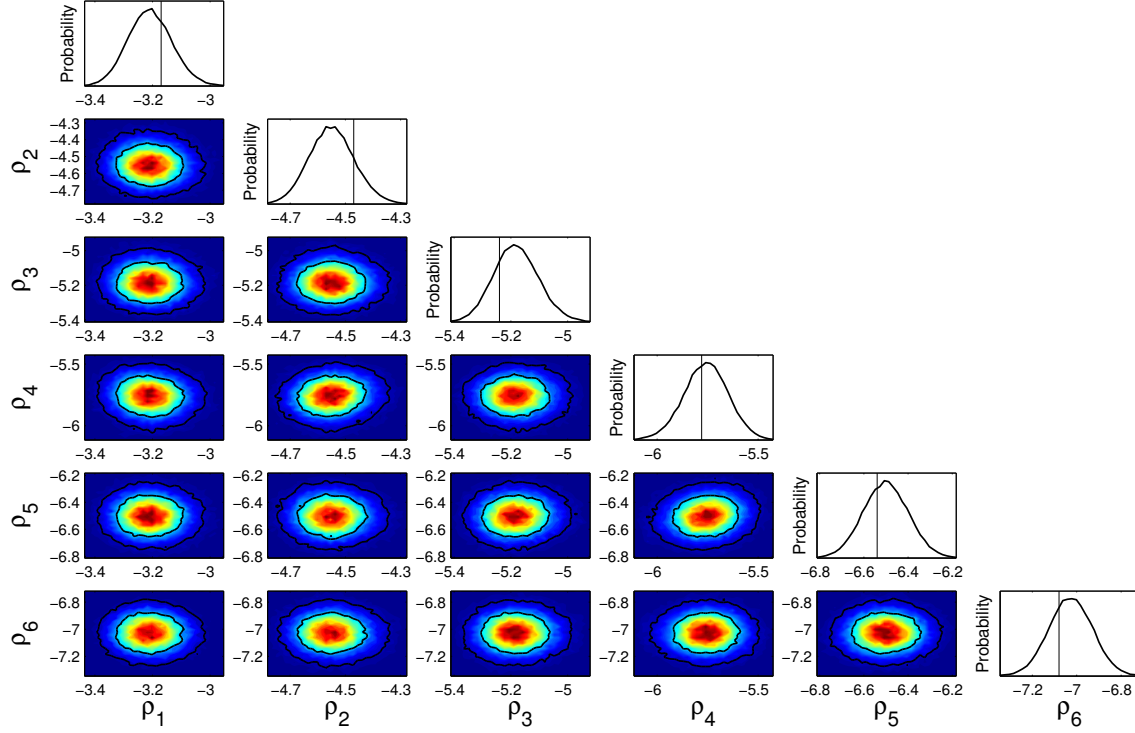


Figure 2. 1D and 2D marginalised posteriors for the six GWB Power Spectrum coefficients $\{\rho_i\}$. The vertical line in the 1D distribution represents the power in the injected background at the frequency of that coefficient. Contours in the 2D plots represent 68 and 95 % confidence levels. All coefficients are consistent with the injected spectrum at the $1 - 2\sigma$ confidence level.

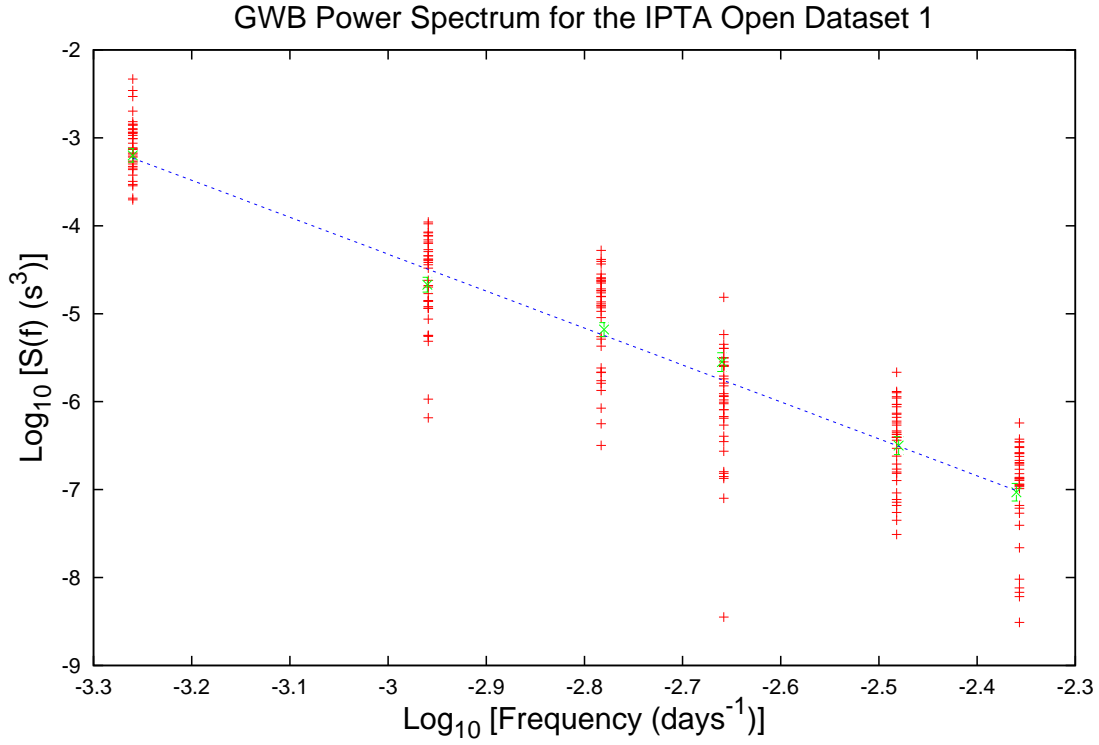


Figure 3. Log-Log Plot of the parameterised GWB power spectrum in Open Dataset 1. The red points represent the power at the sampled frequency for each of the 36 pulsars, whilst the green points represent the marginalised values of the 6 GWB power coefficients $\{\rho_i\}$. The blue dotted line shows the best fit power spectrum to the marginalised coefficients, for which $A_h = (5.05 \pm 0.2) \times 10^{-14}$ and $\alpha = 4.2 \pm 0.12$, consistent with the injected spectrum at $\sim 1 \sigma$ confidence levels.

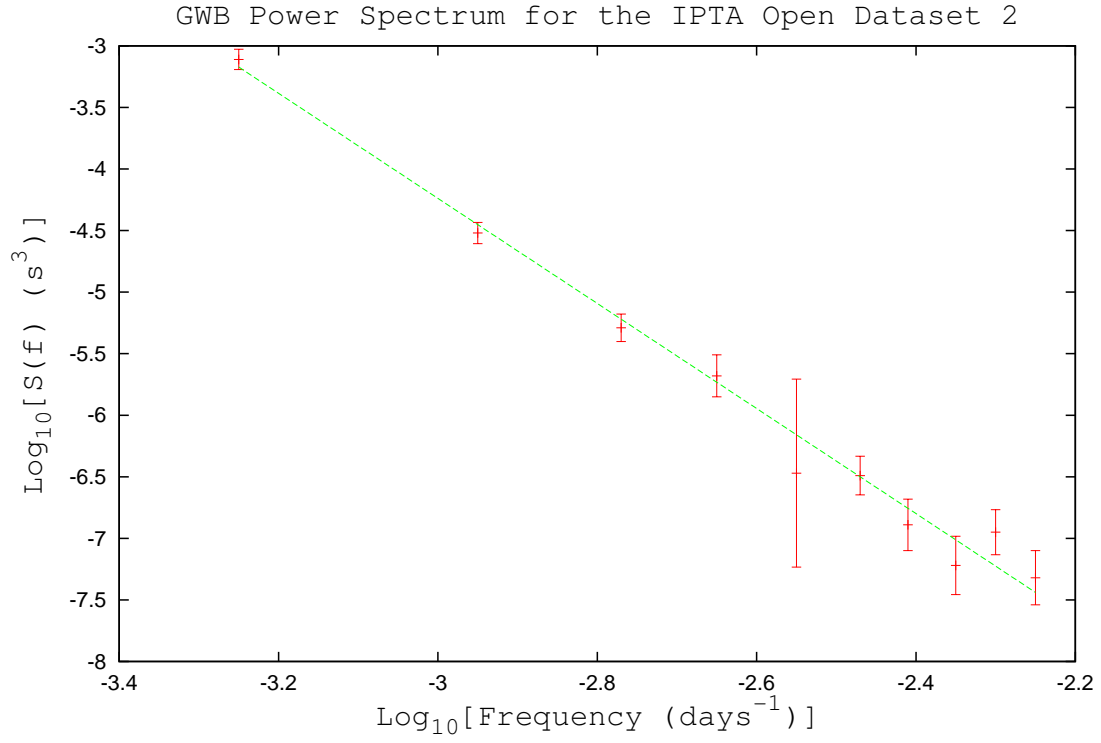


Figure 4. Log-Log Plot of the parameterised GWB power spectrum in Open Dataset 2. The green points represent the marginalised values of the 10 GWB power coefficients $\{\rho_i\}$. The blue dotted line shows the best fit power spectrum to the marginalised coefficients, for which $A_h = (5.4 \pm 0.3) \times 10^{-14}$ and $\alpha = 4.3 \pm 0.12$, consistent with the injected spectrum at $\sim 1 \sigma$ confidence levels.